Chin. J. Astron. Astrophys. Vol. 8 (2008), No. 5, 489–502
(*http://www.chjaa.org*)

Chinese Journal of
Astronomy and
Astrophysics

Resolving the Mass Discrepancy between Strong and Weak Lensing Methods

Qian Zheng

National Astronomical Observatories, Chinese Academy of Sciences, Beijing 100012, China;
zq@bao.ac.cn

Received 2007 December 7; accepted 2008 January 24

Abstract We readdress the outstanding cluster mass discrepancy between strong and weak gravitational lensing techniques utilizing updated data of both giant arcs and weak lensing measurements from the literature. We find that the systematically higher values of cluster masses revealed by strong lensing can be attributed to the oversimplification of the lensing model when estimating the cluster mass enclosed within the giant arcs. This arises because inhomogeneities and substructures in the central cores of clusters may invalidate the spherical symmetry assumption used widely in previous applications. When a more realistic modeling of the arcs is used, then the masses by strong lensing agree fairly well with those given by weak lensing when both are extrapolated to the same cluster regions. We conclude that as of now no significant discrepancy has been found among different cluster mass estimators including optical galaxies, X-ray gas and lensing.

Key words: cosmology: gravitational lensing — galaxies: clusters

1 INTRODUCTION

As the largest virialized system in the universe, clusters of galaxies have been considered to be an ideal laboratory to test theories of structure formation. However, the extent to which clusters can be used for such a purpose depends crucially on how accurately their gravitating masses can be determined from astrophysical observations. The dynamical method based on the measurements of optical galaxies and X-ray emitting gas relies on the equation of state for baryons over the whole cluster regimes, in addition to the requirement of equilibrium and, sometimes, the spherical assumption. With the discovery of arc-like images in the central regions of clusters and the weakly distorted images of distant galaxies in the surrounding regions, gravitational lensing has been proved to be a powerful tool for mapping the mass distribution of clusters that is independent of the underlying mass content and state. This is particularly suited for revealing the existence of dark matter and also for examining the accuracy of dynamical mass estimates.

Since the first detection of a discrepancy between the masses derived by the dynamical method and strong gravitational lensing in several strong lensing clusters (Wu 1994; Miralda-Escude & Babul 1995), there have been many studies of joint determinations and comparisons of cluster masses derived from X-ray, optical galaxies and lensing (e.g. Squires et al. 1996,1997; Smail et al. 1997; Allen 1998; Smith et al. 2005; Auger et al. 2006; Limousin et al. 2007). It turns out that at large radii from the cluster centers, all approaches seem to yield a consistent result. However, at the central regions of the clusters, strong gravitational lensing yields systematically higher cluster masses than do both the dynamical and weak lensing methods. If confirmed, this may cast doubt upon the cosmological applications of cluster masses. Among many other explanations for the discrepancy, inhomogeneities in the invisible matter along the line-of-sight and/or in substructures in the central cores of the clusters are believed to be the most plausible causes, because the configuration of the giant arcs can be easily distorted by matter inhomogeneities of

$10^{14}\ M_{\odot}$. This argument is further supported by the absence of counter arc-like images in most of the strong lensing clusters. It seems that a sophisticated modeling of arc systems including a realistic smooth potential of the cluster, substructures and even baryonic mass components such as central cD galaxies may have to be eventually invoked.

The goal of the present paper is to reexamine the outstanding cluster mass discrepancy as derived with the strong and weak lensing methods. Instead of working with detailed modeling of the numerous individual arc systems, we shall deal with a nonexhaustive catalog of strong and weak clusters by an extensive search of the literature with emphasis on recent observations, and carry out a statistical study of cluster masses reconstructed from both the strong and weak techniques. In particular, for a few tens of clusters we derived the central masses using a modeling of all the available arcs combined with the updated knowledge of the cluster galaxies. This permits a straightforward comparison between cluster masses derived from giant arcs under the assumption of spherical symmetry and from more realistic modeling of arcs. Such a study will help to clarify the issue of whether or not the mass discrepancy reported in the literature is due to the oversimplification of strong lensing model. Either a positive or a negative answer to the question will be of great significance for our understanding of structures and dynamical evolution of galaxy clusters. Throughout the paper, we adopt a concordance cosmological model of $\Omega_m = 0.3$,$\Omega_\Lambda = 0.7$ and $H_0 = 71$ $\mathrm{km\ s^{-1}\ Mpc^{-1}}$.

2 CLUSTER MASS ESTIMATES FROM STRONG AND WEAK LENSING

2.1 Strong Lensing

A quick and simple estimate of the cluster mass enclosed within giant luminous arcs that has been widely used in the literature, is based on two assumptions: (1) Clusters acting as gravitational lenses have a spherical matter distribution; (2) the giant arcs trace essentially the Einstein radii. The lensing equation under these assumptions gives immediately the projected masses within the arc radii $r_{\rm arc}$:

$$m(r < r_{\rm arc}) = \pi r_{\rm arc}^2 \Sigma_{\rm crit}, \tag{1}$$

where the critical surface mass density is defined as $\Sigma_{\rm crit} = (c^2/4\pi G)(D_{\rm s}/D_{\rm d}D_{\rm ds})$, $D_{\rm s}$ and $D_{\rm d}$ are the angular diameter distances from the observer to the source and to the lensing cluster, respectively, and $D_{\rm ds}$ is the angular diameter distance from the cluster to the source. Consequently, one may able to depict the mass distribution in the central regions of clusters provided that a sufficiently large number of arcs are present and that their redshifts are measurable spectroscopically.

While it is very useful, at first sight, to make a quick and rough estimate of gravitating masses of clusters from Equation (1), the results so derived have apparently some drawbacks because of the oversimplification of the underlying matter configurations of clusters. Hereafter, we shall call this method the fiducial model. A more sophisticated treatment of the problem is the so-called mass modeling of arcs, which makes an attempt to constrain the mass profile of clusters by combining all the available data of the positions, shapes, and amplifications of all the lensed images. The more information one has on the arcs, the more robust the cluster mass profile can be reconstructed. Since the essentials of the method are to solve the lensing equation for a number of arcs for a given gravitational potential, this even allows one to probe the very complex configurations including the modeling of substructures and asymmetric matter distributions. In particular, the method has turned to be a very powerful tool for the study of cluster mass distributions nowadays when combined with other observational constraints such as provided by the optical galaxies, X-ray gas, SZ effect and weak gravitational lensing.

2.2 Weak Lensing

In contrast, the weak lensing method studies statistically the weakly distorted images of distant galaxies behind foreground clusters. It probes the mean tangential shear (γ_T) of the lensed galaxies within given radii of the cluster, and then converts γ_T to the convergence parameter κ which measures directly the mass distribution projected along the line-of-sight and weighted by a distance function. To be specific, the projected cluster mass within radius r_0 is given by

$$m(r < r_0) = \pi r_0^2 \zeta(r_0) \Sigma_{\rm crit}, \tag{2}$$

where ζ denotes the difference between the mean projected mass densities within radius r_0 and within the annulus $(r_{\max} - r_0)$ (e.g., Fahlman et al. 1994):

$$\zeta(r_0) = 2\left(1 - r_0^2/r_{\max}^2\right)^{-1} \int_{r_0}^{r_{\max}} \langle\gamma_{\rm T}\rangle d\ln r = \overline{\sigma}(r < r_0) - \overline{\sigma}(r_0 < r < r_{\max}), \quad (3)$$

where $r_{\max}$ denotes the outer boundary of the data, and $\overline{\sigma}(r < r_0)$ and $\overline{\sigma}(r_0 < r < r_{\max})$, the mean surface mass density interior to r_0 and within the annulus $r_0 < r < r_{\max}$. In the limit of $r_{\max} \gg r_0$, we may neglect the second term and obtain a tight constraint on $m(r < r_0)$.

3 SAMPLE

We drew up a nonexhaustive catalog of both strong and weak lensing clusters by an extensive search of the literature with emphasis on recent observations. This resulted in a total of 59 strong lensing clusters containing 97 arc-like images and 75 weak lensing clusters. Their properties are summarized in Tables 1–3, respectively. The mean redshift of the lensing clusters is approximately $\langle z_{\rm d}\rangle \simeq 0.3$. An examination of the relationship between the velocity dispersion σ of the optical galaxies and the temperature T of the X-ray emitting gas, where available, for 99 lensing clusters (see Fig. 1) gives

$$(\sigma/{\rm km\,s^{-1}}) = 10^{2.56^{+0.15}_{-0.14}} ({\rm kT/keV})^{0.54^{+0.09}_{-0.08}}. \quad (4)$$

The global properties of these lensing clusters are therefore consistent with the scenario that these systems are more or less dynamically relaxed.

For the giant arcs whose redshifts are not observationally available, we assume a mean redshifts of $\langle z_{\rm s}\rangle = 0.8$ except for the arcs in MS1137 ($\langle z_{\rm d}\rangle = 0.782$) in which a value of $\langle z_{\rm s}\rangle = 2.0$ is adopted for the arcs without redshift measurements. The critical density $\Sigma_{\rm crit}$ differs only by a factor of 1.4 between these two redshifts for a cluster at $\langle z_{\rm d}\rangle = 0.3$. To ensure that the arc-like images are the most strongly distorted events and therefore trace as closely as possible the Einstein radii in the associated lensing clusters, we

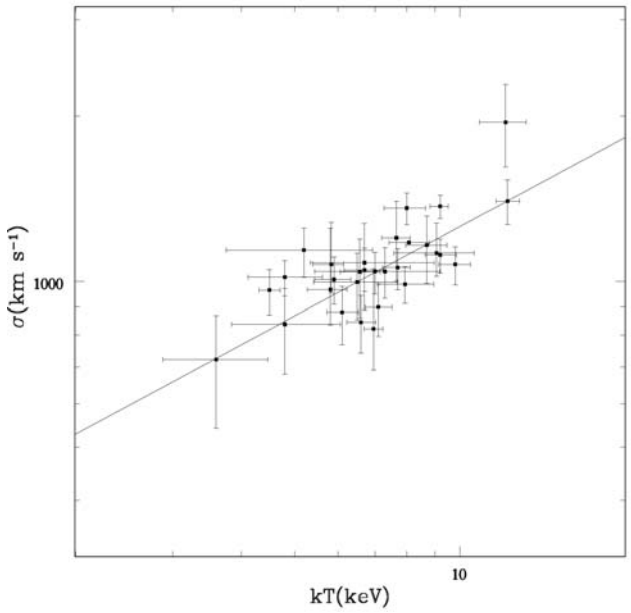

Fig. 1 The σ-T relationship of the lensing clusters for which both velocity dispersion σ and X-ray temperature T are observationally available. The solid line is the best fit to the data: $(\sigma/{\rm km\,s^{-1}}) = 10^{2.56^{+0.15}_{-0.14}} ({\rm kT/keV})^{0.54^{+0.09}_{-0.08}}$ (33 clusters).

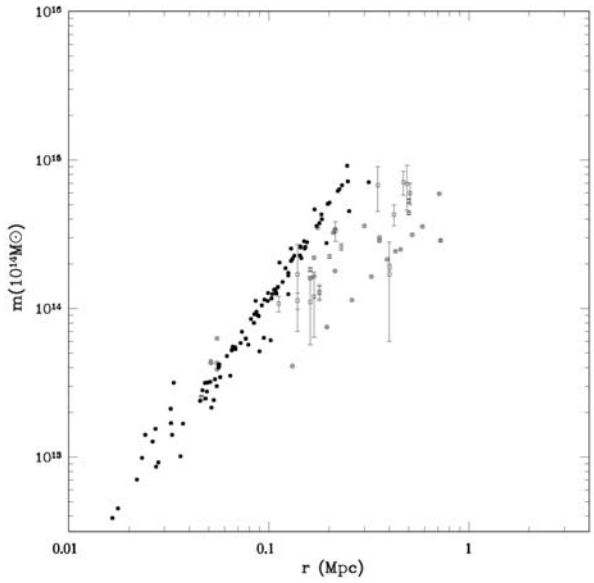

Fig. 2 Comparison of cluster mass estimates determined from the fiducial model (filled circles, 59 clusters) and the modeling of arcs (open squares,10 clusters).

require that all the tangential arcs in this analysis should have their length-to-width ratios greater than 10, a condition for selection of giant arcs (Wu & Hammer 1993). In Table 1, we list all the values of cluster masses enclosed within the arc-like images determined by our fiducial model, Equation (1). We also display in Figure 2 a plot of the determined mass against the arc radius for all the clusters. It appears that the overall projected cluster masses follow a power-law of $\sim r^{-2}$.

We have selected 10 lensing clusters for which a sophisticated modeling of arcs has been carried out by different authors (Table 2). These include both fully relaxed and unrelaxed clusters, distinguished by whether or not significant substructures are presented. The cluster masses have been taken directly from the literature (see Table 2) and shown in Figure 2 (open squares).

A total of 75 weak lensing clusters were chosen (Table 3). Many of the clusters contain more than one measurement made at different radii. The mean cluster mass density with respect to cosmic background are given at varous radii (e.g. r_{180}, r_{200} or r_{500}), which have been converted to physical units from the cosmic virial theorem. The resultant masses are plotted versus the radii for the 75 clusters in Figure 3.

4 RESULTS

Comparisons between cluster masses determined by strong and weak lensing are made in a very straightforward manner. The first question we attempt to answer is whether the cluster masses derived from the two strong lensing approaches agree with each other. This is achieved by the combined plot shown in Figure 2. An immediate conclusion one can draw from this simple statistical comparison is that the masses given by the fiducial model are systematically higher than the values given by the modeling of arc systems. The latter is believed to be a more plausible estimator of the cluster mass, and the oversimplification in our fiducial model resulting from the assumptions of a smooth spherical mass distribution and of the arc tracing the Einstein radius may have led to a biased, high cluster mass. However, this does not diminish the value of the fiducial model as a quick and rough estimator of the cluster mass enclosed within giant arcs.

When we compare the cluster masses given by strong lensing and by weak lensing (see Fig. 4), we find a similar trend: The fiducial model yields an overestimate of cluster masses if the weak lensing data are extrapolated to the inner cluster cores. In contrast, a fairly good agreement of cluster mass estimates is found between the modeling of strong lensing events and the weak lensing algorithm. Taking these observational

Table 1 Strong Lensing Cluster Sample I

Cluster	$z_{\rm cluster}$	T (keV)	σ	$z_{\rm arc}$	$r_{\rm arc}$(Mpc)	$m(10^{14}M_{\odot})$	References
A68	0.255	$8.0^{+0.8}_{-0.6}$	1360^{+89}_{-92}	...	0.152	2.593	[16,19,24,25]
				...	0.089	0.890	[24,25]
A114	0.312	...	904	...	0.103	1.17	[6,17,18]
				...	0.151	2.54	[6,17,18]
A118	0.308	...	...	...	0.0088	0.0086	[23]
				...	0.117	1.511	[23]
A209	0.206	$7.10^{+0.40}_{-0.40}$	898^{+92}_{-102}	...	0.0680	0.553	[16,19,23]
A370	0.375	$7.2^{+0.8}_{-0.8}$	...	0.724	0.221	6.198	[2,16,26]
				...	0.108	1.351	[2,26]
				...	0.104	1.249	[2,26]
				0.725	0.246	9.155	[2,26]
				1.30	0.113	2.04	[2,26]
A383	0.187	...	701^{+138}_{-171}	1.01	0.0453	0.239	[16,22]
				...	0.0653	0.527	[22]
				...	0.0509	0.321	[22]
A586	0.17	$6.96^{+0.99}_{-0.83}$	...	1.43	0.0766	0.6267	[10,19,23]
				0.61	0.0563	0.4112	[10]
A773	0.2170	$8.07^{+0.70}_{-0.66}$	...	0.650	0.0814	0.850	[5,19,23]
				...	0.184	3.990	[23]
A869	0.153	...	...	...	0.0479	0.31	[23]
A963	0.206	$6.6^{+0.4}_{-0.4}$	844^{+99}_{-102}	0.771	0.0372	0.168	[11,16,19,23]
				1.958	0.0548	0.300	[11,23]
				...	0.0678	0.549	[11,23]
A1137	0.782	$5.7^{+1.3}_{-0.7}$	...	...	0.125	1.249	[23]
A1204	0.155	$3.8^{+0.2}_{-0.2}$	...	...	0.0219	0.0704	[28]
A1682	0.221	$6.42^{+0.63}_{-0.60}$	...	...	0.155	2.793	[19,23]
A1689	0.183	$9.2^{+0.4}_{-0.3}$	1370^{+65}_{-68}	1.83	0.109	1.259	[16,23]
				3.05	0.145	2.186	[23]
				...	0.131	2.164	[23]
				...	0.129	2.090	[23]
				...	0.225	6.375	[23]
				...	0.134	2.265	[23]
				...	0.150	2.835	[23]
				...	0.144	2.613	[23]
				...	0.129	2.535	[23]
A1835	0.253	$7.42^{+0.61}_{-0.43}$	...	...	0.111	1.396	[19,23]
A1914	0.1712	$10.53^{+0.51}_{-0.50}$	...	...	0.0733	0.698	[5,23]
A1942	0.224	...	...	...	0.0262	0.127	[28]
A2104	0.155	$9.13^{+0.69}_{-0.45}$	1201^{+200}_{-200}	...	0.0176	0.0451	[9,19,28]
A2163	0.2080	$12.3^{+1.3}_{-1.1}$	1698	0.728	0.0465	0.282	[9,28]
A2218	0.1756	$7.0^{+0.40}_{-0.30}$	1042^{+87}_{-94}	0.702	0.0563	0.421	[5,16,20,23]
				1.034	0.173	3.592	[20,23]
				...	0.066	0.554	[20,23]
				...	0.201	5.170	[20,23]
				...	0.095	1.148	[20,23]
				...	0.121	1.867	[20,23]
A2219	0.2280	$9.8^{+0.7}_{-0.6}$	1074^{+82}_{-89}	1.070	0.0571	0.345	[5,16,19,23]
				2.730	0.0789	0.572	[23]
A2259	0.164	...	...	1.477	0.0273	0.0861	[23]
A2261	0.224	$665^{+0.49}_{-0.48}$	...	...	0.088	0.904	[19,23]
A2280	0.228	...	948^{+516}_{-285}	...	0.0563	0.415	[28]
A2294	0.178	...	...	...	0.0866	0.953	[23]
A2390	0.2280	$9.2^{+0.6}_{-0.6}$	1117^{+76}_{-82}	1.033	0.125	1.674	[14,16,20]
				0.913	0.125	1.737	[14,20]
				...	0.028	0.092	[14,20]
				...	0.049	0.276	[14,20]
A2397	0.224	...	...	...	0.0492	0.317	[28]

Table 1 – Continued.

Cluster	$z_{\rm cluster}$	T (keV)	σ	$z_{\rm arc}$	$r_{\rm arc}$(Mpc)	$m(10^{14}M_{\odot})$	References
A2667	0.2264	...	...	1.034	0.0483	0.248	[16,23,26]
				...	0.0537	0.334	[23,26]
A2744	0.3080	$12.1^{+1.4}_{-1.0}$	1950^{+334}_{-334}	...	0.0842	0.800	[5,28]
3C220	0.620	...	...	1.49	0.052	0.242	[8,23]
3C295	0.299	...	907	...	0.0232	0.0986	[28]
				0.93	0.0986	1.127	[28]
Cl0024	0.395	$5.2^{+2.0}_{-1.3}$	1140^{+111}_{-123}	...	0.179	3.754	[4,8,16]
				...	0.248	7.184	[4,8]
Cl0302	0.423	...	1100	...	0.0859	1.127	[28]
Cl0500	0.327	$7.2^{+3.7}_{-1.8}$	...	0.913	0.106	1.338	[28]
Cl2236	0.552	...	...	1.116	0.0617	0.479	[28]
Cl2244	0.330	$7.10^{+5.00}_{-2.20}$	...	2.237	0.0361	0.101	[23]
				...	0.143	2.271	[23]
				2.37	0.0328	0.141	[23]
MS0440	0.19	$5.3^{+1.3}_{-0.8}$	...	0.53	0.065	0.524	[23]
MS0955	0.145	...	...	...	0.0271	0.155	[28]
MS1006	0.261	...	906^{+101}_{-101}	...	0.056	0.401	[28]
				...	0.099	1.27	[28]
				...	0.197	5.070	[28]
MS1008	0.306	$7.3^{+2.5}_{-1.5}$	1042^{+110}_{-110}	...	0.183	4.296	[28]
MS1358	0.3290	$6.7^{+0.6}_{-0.5}$	1048^{+102}_{-89}	4.92	0.0943	0.635	[13,16]
MS1455	0.2568	$4.5^{+0.2}_{-0.2}$	964^{+87}_{-95}	...	0.0722	0.586	[16,23]
MS1621	0.4275	$6.5^{-1.3}_{-1.0}$	997^{+128}_{-146}	...	0.0324	0.169	[16,28]
MS1910.5	0.246	...	...	...	0.232	6.761	[28]
MS2053	0.58	$8.1^{+3.7}_{-2.2}$	...	3.146	0.0897	0.514	[6,27]
MS2137	0.313	$4.4^{+0.4}_{-0.4}$	960	1.501	0.0641	0.353	[7,21,23]
MS2318	0.130	5.1	...	...	0.0845	0.915	[28]
GH02154	0.320	...	...	0.721	0.0241	0.141	[28]
PKS0745	0.103	$8.5^{+1.6}_{-1.2}$	...	0.433	0.0323	0.2113	[28]
RXJ0451	0.430	$10.6^{+1.6}_{-1.3}$	...	2.007	0.194	2.764	[8]
				...	0.144	2.581	[8]
RXJ1133	0.349	...	...	1.544	0.0516	0.215	[22]
RXJ1347	0.451	$12.2^{+0.6}_{-0.6}$	1400^{+130}_{-130}	...	0.169	4.648	[28]
GC03053	0.43	...	...	...	0.0922	1.050	[23]
Zw3146	0.291	$680^{+0.38}_{-0.36}$	...	...	0.108	1.303	[19,23]
Zw3179	0.143	...	...	...	0.0165	0.0389	[23]
RCS0224	0.77	...	...	4.879	0.102	0.612	[15,23]
SDSS+26.733	0.44	...	886.787	$0.61^{+0.14}_{-0.14}$	0.0334	0.3166	[12]
SDSSJ002240	0.38	...	420^{+70}_{-70}	2.73	0.0111	0.0124	[1]
1ES0657	0.296	...	1400^{+100}_{-100}	3.24	0.2518	4.520	[3]
				3.24	0.3153	7.089	[3]

References: [1] Allam et al. (2007); [2] Bezecourt et al. (1999); [3] Bradac et al. (2006); [4] Broadhurst et al. (2000); [5] Cassano et al. (2007); [6] Campusano et al. (2001); [7] Clowe et al. (2003); [8] Comerford et al. (2006); [9] Cypriano et al. (2003); [10] Cypriano et al. (2005); [11] Ellis et al. (1991); [12] Estrada et al. (2007); [13] Franx et al. (1997); [14] Frye et al. (1998); [15] Gladders et al. (2002); [16] Hoekstra (2007); [17] Lemoine-Busserolle et al. (2003); [18] Mellier et al. (1991); [19] Pedersen (2007); [20] Pello et al. (2000); [21] Sand et al. (2002); [22] Sand et al. (2004); [23] Sand et al. (2005); [24] Smith et al. (2001); [25] Smith et al. (2002); [26] Soucail et al. (1988); [27] Tran et al. (2005); [28] Wu et al. (1998).

facts as a whole, we can attribute the long outstanding mass discrepancy between strong lensing in terms of the fiducial model and weak lensing to the inaccuracy of the strong lensing model used widely in the literature. The failure of our fiducial model indicates that cluster mass distribution may deviate significantly from a smooth, spherical density profile. In particular, giant arcs are produced mainly by matter within the central cores of clusters and therefore, any sufficiently large substructures and asymmetrical matter structures can easily introduce perturbations to the arc-like images. Indeed, this is further supported by the

Table 2 Strong Lensing Cluster Sample II

Cluster	$z_{\rm cluster}$	T (keV)	σ	r(Mpc)	$m(10^{14}M_{\odot})$	References
A68	0.255	$8.0^{+0.8}_{-0.6}$	1360^{+89}_{-92}	0.5	$5.31^{+0.17}_{-0.17}$	[16]
				0.5	$4.4^{+0.1}_{-0.1}$	[16]
A114	0.312	...	904	0.429	2.43	[12]
				0.357	2.86	[12]
A370	0.375	$7.2^{+0.8}_{-0.8}$	...	0.214	3.43	[3,18]
A383	0.187	...	701^{+138}_{-171}	0.046	$0.25^{+0.01}_{-0.01}$	[17]
				0.179	$1.27^{+0.14}_{-0.14}$	[17]
				0.046	$0.25^{+0.007}_{-0.007}$	[17]
				0.179	$1.3^{+0.14}_{-0.14}$	[17]
A586	0.17	$6.96^{+0.99}_{-0.83}$	...	0.422	$4.3^{+0.7}_{-0.7}$	[6]
A1689	0.183	$9.2^{+0.4}_{-0.3}$	1370^{+65}_{-68}	0.175	3.5	[6]
				0.35	$6.76^{+2.25}_{-2.25}$	[6]
				0.21	3.24	[6]
				0.3	3.6	[6]
				0.23	$2.6^{+0.14}_{-0.14}$	[21]
				0.47	$7.1^{+1.29}_{-1.29}$	[19]
				0.49	$6.9^{+2.29}_{-2.29}$	[8]
				0.507	$6.0^{+1.0}_{-1.0}$	[6]
A2218	0.1756	$7.0^{+0.40}_{-0.30}$	1042^{+87}_{-94}	0.0513	0.44	[11]
				0.0513	0.44	[11]
				0.0513	0.43	[2]
				0.055	0.43	[10]
				0.055	0.39	[2]
				0.055	0.63	[1]
A2219	0.2280	$9.8^{+0.7}_{-0.6}$	1074^{+82}_{-89}	0.131	0.41	[4]
				0.195	0.75	[4]
				0.26	1.14	[4]
				0.325	1.64	[4]
				0.39	2.14	[4]
				0.455	2.5	[4]
				0.52	3.14	[4]
				0.585	3.57	[4]
				0.71	5.93	[4]
				0.214	1.79	[4]
				0.357	3.0	[4]
A2390	0.2280	$9.2^{+0.6}_{-0.6}$	1117^{+76}_{-82}	0.139	$1.7^{+1.0}_{-1.0}$	[7]
				0.139	$1.13^{+0.14}_{-0.14}$	[14]
				0.112	$1.08^{+0.13}_{-0.13}$	[13]
Cl0024	0.395	$5.2^{+2.0}_{-1.3}$	1140^{+111}_{-123}	0.161	$1.83^{+0.06}_{-0.06}$	[5]
				0.168	$2.20^{+0.003}_{-0.003}$	[20]
				0.161	1.59	[7]
				0.168	1.65	[7]
				0.161	$1.11^{+0.54}_{-0.54}$	[7]
				0.168	$1.20^{+0.56}_{-0.56}$	[7]
				0.201	$2.24^{+0.06}_{-0.06}$	[22]
				0.215	$3.34^{+0.51}_{-0.51}$	[20]
RCS0224	0.77	...	...	0.4	$1.9^{+0.1}_{-0.1}$	[15]
				0.4	$1.7^{+1.1}_{-1.1}$	[15]
MS2137	0.313	$4.4^{+0.4}_{-0.4}$	960	1.26	7.75	[13]

References: [1] Abdelsalam et al. (1998); [2] Allen et al. (1998); [3] Bezecourt et al. (1999); [4] Bezecourt et al. (2000); [5] Broadhurst et al. (2000); [6] Diego et al. (2005); [7] Diaferio et al. (2005); [8] Dye et al. (2001); [9] Gravazzi et al. (2003); [10] Kneib et al. (1995); [11] Loeb et al. (1994); [12] Natarajan et al. (1998); [13] Pierre et al. (1995); [14] Pierre et al. (1996); [15] Rzepecki et al. (2007); [16] Richard et al. (2007); [17] Smith et al. (2001); [18] Soucail et al. (1988); [19] Taylor et al. (1998); [20] Tyson et al. (1998); [21] Zekser et al. (2006); [22] Zhang et al. (2005).

Table 3 Weak Lensing Cluster Sample

Cluster	$z_{\rm cluster}$	T (keV)	σ	r(Mpc)	$m(10^{14}M_{\odot})$	References
A68	0.255	$8.0^{+0.8}_{-0.6}$	1360^{+89}_{-92}	0.39	3.51	[14]
				1.618	$30.10^{+9.56}_{-10.14}$	[20]
				0.704	$6.197^{+1.127}_{-1.127}$	[13]
A114	0.312	...	904	0.352	$3.093^{+1.307}_{-1.307}$	[22]
A115	0.197	$5.83^{+0.47}_{-0.30}$	1074^{+208}_{-121}	1.65	$3.408^{+3.296}_{-2.592}$	[15,20]
				2.38	$8.465^{+5.83}_{-5.83}$	[7]
A118	0.308	...	...	0.282	$2.919^{+1.401}_{-1.401}$	[22]
A209	0.206	$7.10^{+0.40}_{-0.40}$	898^{+92}_{-102}	0.39	1.25	[14]
				0.704	$5.493^{+1.268}_{-1.268}$	[13]
				1.647	$10.620^{+5.972}_{-5.451}$	[20]
				$2.243^{+0.243}_{-0.243}$	$10.271^{+2.914}_{-2.914}$	[2]
A267	0.230	$5.9^{+0.5}_{-0.4}$	1008^{+99}_{-99}	0.39	2.06	[14]
				0.704	$4.648^{+0.845}_{-0.845}$	[13]
				1.633	$12.38^{+4.04}_{-4.97}$	[20]
				2.354	$16.620^{+6.141}_{-6.141}$	[7]
A370	0.375	$7.2^{+0.8}_{-0.8}$	...	0.704	$9.155^{+1.268}_{-1.268}$	[13]
A383	0.187	...	701^{+138}_{-171}	0.39	2.80	[14]
				0.704	$3.662^{+0.986}_{-0.986}$	[13]
				2.20	11.2	[14]
				$1.886^{+0.243}_{-0.243}$	$5.986^{+2.086}_{-2.086}$	[2]
A520	0.2010	$7.94^{+0.96}_{-0.90}$	988^{+76}_{-76}	1.649	$12.211^{+4.732}_{-3.662}$	[3,20]
				2.377	$18.352^{+6.310}_{-6.310}$	[7]
A586	0.17	$6.96^{+0.99}_{-0.83}$	...	2.405	$37.75^{+12.52}_{-12.52}$	[7]
				1.668	$35.592^{+9.873}_{-11.423}$	[20]
A611	0.288	$6.85^{+0.48}_{-0.46}$	...	1.599	$5.39^{+4.211}_{-3.930}$	[20]
				2.305	$7.338^{+4.887}_{-4.887}$	[7]
A665	0.1816	$6.96^{+0.28}_{-0.27}$	821^{+233}_{-130}	2.395	$11.65^{+6.619}_{-6.619}$	[3,7]
A697	0.282	$10.2^{+0.8}_{-0.8}$	1334^{+114}_{-95}	2.310	$28.73^{+10.34}_{-10.34}$	[7,10]
A773	0.2170	$8.07^{+0.70}_{-0.66}$	1177	0.39	4.01	[3,14]
				2.366	$17.0^{+7.577}_{-7.577}$	[7]
A781	0.29	$7.3^{+1.1}_{-0.7}$	674^{+43}_{-52}	2.295	$14.085^{+6.408}_{-6.408}$	[7]
A959	0.285	$5.24^{+0.89}_{-0.73}$	...	1.601	$13.141^{+4.930}_{-4.930}$	[19]
				1.89	19.2	[6]
A963	0.206	$6.6^{+0.4}_{-0.4}$	844^{+99}_{-102}	0.39	2.58	[14]
				0.704	$3.803^{+0.845}_{-0.845}$	[13]
				2.375	$9.366^{+8.18}_{-8.18}$	[7]
				$1.90^{+0.143}_{-0.143}$	$5.657^{+1.286}_{-1.286}$	[2]
A1137	0.782	$5.7^{+1.3}_{-0.7}$	...	0.49	$8.9^{+0.39}_{-1.8}$	[4]
A1423	0.21	...	...	2.37	$16.620^{+8.37}_{-8.37}$	[7]
A1576	0.299	$6.57^{+0.56}_{-0.54}$	1041^{+153}_{-183}	1.592	$12.141^{+4.789}_{-3.577}$	[20]
				2.295	$20.408^{+6.563}_{-6.563}$	[7]
A1682	0.221	$6.42^{+0.63}_{-0.60}$	...	1.635	$3.155^{+2.676}_{-1.873}$	[20]
				2.358	$6.169^{+4.113}_{-4.113}$	[7]
A1689	0.183	$9.2^{+0.4}_{-0.3}$	1370^{+65}_{-68}	0.704	$9.437^{+0.986}_{-0.986}$	[13]
				$1.80^{+0.08}_{-0.55}$	$18.0^{+4.0}_{-7.0}$	[19]
				$1.50^{+0.11}_{-0.12}$	$17.0^{+3.0}_{-2.0}$	[19]
				$3.214^{+0.20}_{-0.20}$	$28.157^{+4.80}_{-4.80}$	[24]
A1722	0.325	$5.81^{+0.59}_{-0.39}$	966^{+283}_{-132}	1.577	$3.803^{+3.014}_{-2.225}$	[20]
A1758N	0.280	$6.88^{+0.86}_{-0.75}$	...	1.604	$28.690^{+8.972}_{-9.366}$	[20]
A1763	0.223	$7.7^{+0.5}_{-0.4}$	1060^{+87}_{-95}	0.39	1.66	[14]
				1.634	$6.9^{+3.408}_{-4.324}$	[20]
				2.36	$11.746^{+5.662}_{-5.662}$	[7]
				$2.757^{+0.20}_{-0.20}$	$19.80^{+3.757}_{-3.757}$	[2]

Table 3 – Continued.

Cluster	$z_{\rm cluster}$	T (keV)	σ	r(Mpc)	$m(10^{14}M_{\odot})$	References
A1835	0.253	$7.42^{+0.61}_{-0.43}$	...	0.39	4.62	[14]
				2.335	$11.817^{+6.239}_{-6.239}$	[7]
				$3.414^{+0.20}_{-0.20}$	$38.67^{+5.914}_{-5.914}$	[2]
A1914	0.1712	$10.53^{+0.51}_{-0.50}$	...	1.668	$3.690^{+2.859}_{-2.718}$	[3,20]
				2.404	$10.141^{+6.211}_{-6.211}$	[7]
A1995	0.320	$9.06^{+1.77}_{-1.32}$	1126^{+151}_{-105}	1.580	$33.37^{+9.69}_{-8.63}$	[20]
A2104	0.155	$9.13^{+0.69}_{-0.45}$	1201^{+200}_{-200}	1.678	$19.92^{+7.52}_{-7.82}$	[20]
A2111	0.229	$6.94^{+0.76}_{-0.76}$	...	2.354	$6.873^{+4.014}_{-4.014}$	[7]
				1.634	$5.408^{+2.54}_{-3.01}$	[20]
A2163	0.2080	$12.3^{+1.3}_{-1.1}$	1698	0.197	$1.134^{+0.846}_{-0.846}$	[3,23]
				0.641	$11.488^{+8.512}_{-8.512}$	[5,22]
A2204	0.152	$6.68^{+0.28}_{-0.27}$	...	1.679	$11.07^{+7.44}_{-6.44}$	[20]
				2.420	$11.775^{+7.310}_{-7.310}$	[5,7]
A2218	0.1756	$7.0^{+0.40}_{-0.30}$	1042^{+87}_{-94}	0.39	4.33	[14]
				0.704	$6.338^{+0.986}_{-0.986}$	[13]
				0.563	$6.187^{+3.013}_{-3.013}$	[23]
				0.285	$1.667^{+0.813}_{-0.813}$	[23]
				0.274	$1.5^{+0.27}_{-0.27}$	[21]
				0.576	$5.6^{+1.0}_{-1.0}$	[22]
				$2.586^{+0.20}_{-0.20}$	$13.87^{+3.07}_{-3.07}$	[2]
A2219	0.2280	$9.8^{+0.7}_{-0.6}$	1074^{+82}_{-89}	0.39	2.69	[3,9]
				0.704	$7.042^{+0.986}_{-0.986}$	[13]
				1.634	$6.648^{+3.310}_{-4.141}$	[20]
				$1.85^{+0.12}_{-0.13}$	$11.7^{+2.4}_{-2.3}$	[12]
				2.358	$9.155^{+6.254}_{-6.254}$	[7]
				$3.214^{+0.257}_{-0.257}$	$29.914^{+6.214}_{-6.214}$	[2]
A2261	0.224	$665^{+0.49}_{-0.48}$	...	2.358	$9.155^{+6.254}_{-6.254}$	[7]
A2263	0.208	...	...	0.613	$4.37^{+3.13}_{-3.13}$	[23]
A2390	0.2280	$9.2^{+0.6}_{-0.6}$	1117^{+76}_{-82}	1.07	$6.48^{+1.97}_{-1.97}$	[22]
				0.507	2.54	[22]
				0.704	$7.324^{+0.845}_{-0.845}$	[13]
				2.356	$16.887^{+7.437}_{-7.437}$	[7]
				0.139	1.20	[8]
				0.141	$1.282^{+0.658}_{-0.658}$	[22]
				0.358	$2.944^{+1.655}_{-1.655}$	[22]
				0.810	$16.223^{+9.776}_{-9.776}$	[22]
				0.662	$8.488^{+5.512}_{-5.512}$	[22]
				4.7	25.7	[8]
				0.148	$2.4^{+0.15}_{-0.41}$	[8]
				0.176	$1.73^{+0.38}_{-0.22}$	[8]
				0.183	$1.55^{+0.39}_{-1.27}$	[8]
				0.268	$1.73^{+0.81}_{-0.25}$	[8]
				0.289	$2.8^{+1.43}_{-1.0}$	[8]
				0.338	$2.8^{+1.4}_{-1.1}$	[8]
				0.451	$2.96^{+0.24}_{-0.86}$	[8]
				0.56	$3.8^{+2.4}_{-1.5}$	[8]
				0.62	$7.0^{+4.3}_{-3.6}$	[8]
				0.76	$9.0^{+5.1}_{-2.8}$	[8]
				0.94	$18.3^{+5.6}_{-5.0}$	[8]
A2552	0.30	...	...	2.295	$5.211^{+4.10}_{-4.10}$	[7]
A2631	0.28	...	...	2.312	$6.873^{+4.69}_{-4.69}$	[7]

Table 3 – Continued.

Cluster	$z_{\rm cluster}$	T (keV)	σ	r (Mpc)	$m(10^{14}\,M_{\odot})$	References
A2744	0.3080	$12.1^{+1.4}_{-1.0}$	1950^{+334}_{-334}	0.282	$2.879^{+1.36}_{-1.36}$	[3,23]
3C295	0.299	...	907	0.282	$3.707^{+1.75}_{-1.75}$	[23]
3C324	1.206	...	...	0.352	4.225	[23]
3C336	...	...	...	0.352	$3.842^{+1.958}_{-1.958}$	[23]
Cl0024	0.395	$5.2^{+2.0}_{-1.3}$	1140^{+111}_{-123}	0.704	$7.746^{+1.268}_{-1.268}$	[12]
				2.113	28.169	[23]
				0.282	$2.51^{+1.249}_{-1.249}$	[23]
				0.303	3.4	[8]
Cl0054	0.56	...	...	0.282	$2.88^{+1.82}_{-1.82}$	[23]
Cl0303+17	0.0349	...	1079^{+235}_{-235}	0.282	0.310	[23]
Cl0412	0.51	...	...	0.282	0.3521	[23]
Cl601	0.54	...	1166	0.282	1.085	[23]
Cl0939	0.4510	$6.7^{+1.7}_{-1.7}$	1081^{+194}_{-194}	0.528	$4.74^{+2.26}_{-2.26}$	[23]
Cl1040-1155	0.70	...	418^{+55}_{-46}	1.0	<2.2	[16]
Cl1216-1201	0.79	$4.8^{+0.8}_{-0.7}$	1018^{+73}_{-77}	1.0	$5.4^{+1.2}_{-1.2}$	[16]
MS0016	0.5465	$8.7^{+0.8}_{-0.7}$	1164^{+151}_{-173}	0.49	$11.0^{+1.1}_{-1.1}$	[4]
				0.704	$11.13^{+1.55}_{-1.55}$	[13]
				0.282	2.634	[23]
MS0906	0.1704	$6.1^{+0.4}_{-0.4}$	880^{+99}_{-111}	0.704	$5.211^{+0.986}_{-0.986}$	[13]
MS1008	0.306	$7.3^{+2.5}_{-1.5}$	1042^{+110}_{-110}	0.714	3.72	[23]
				4.14	14.3	[23]
MS1054.4	0.833	$10.5^{+3.4}_{-2.1}$	...	0.49	$17.6^{+10.4}_{-5.4}$	[4]
				0.352	$4.34^{+2.26}_{-2.26}$	[23]
				0.704	$9.48^{+4.92}_{-4.92}$	[23]
				1.338	$22.26^{+11.34}_{-11.34}$	[23]
				0.70	$12.8^{+1.3}_{-1.3}$	[18]
				0.70	$17.04^{+2.11}_{-2.11}$	[18]
				0.70	$15.07^{+1.7}_{-1.7}$	[18]
MS1224	0.3225	$4.8^{+1.2}_{-1.0}$	837^{+133}_{-158}	0.704	$4.225^{+1.268}_{-1.268}$	[13]
				1.08	4.93	[2]
				0.676	4.930	[23]
MS1358	0.3290	$6.7^{+0.6}_{-0.5}$	1048^{+102}_{-89}	$0.96^{+0.08}_{-0.10}$	$2.0^{+0.6}_{-0.6}$	[12]
				1.056	$3.44^{+1.56}_{-1.56}$	[8,11]
				0.089	$0.286^{+0.134}_{-0.076}$	[8]
				0.127	$0.54^{+0.16}_{-0.22}$	[8]
				0.155	$0.70^{+0.29}_{-0.16}$	[8]
				0.20	$0.85^{+0.42}_{-0.29}$	[8]
				0.30	$1.27^{+0.55}_{-0.28}$	[8]
				0.42	$1.55^{+0.7}_{-0.42}$	[8]
				0.56	$1.55^{+1.27}_{-0.56}$	[8]
				0.75	$2.82^{+2.28}_{-1.13}$	[8]
				3.6	10.0	[8]
				3.52	9.86	[8]
				3.52	$9.15^{+3.9}_{-3.9}$	[8]
MS1455	0.2568	$4.5^{+0.2}_{-0.2}$	964^{+87}_{-95}	1.617	$4.521^{+3.085}_{-2.507}$	[20]
				2.332	$14.310^{+6.630}_{-6.634}$	[7]
MS1512	0.3727	$3.6^{+0.9}_{-0.7}$	722^{+145}_{-181}	0.704	$2.958^{+1.127}_{-1.127}$	[13]
MS1621	0.4275	$6.5^{-1.3}_{-1.0}$	997^{+128}_{-146}	0.704	$7.464^{+1.408}_{-1.408}$	[13]
MS2053	0.58	$8.1^{+3.7}_{-2.2}$	...	$1.07^{+0.13}_{-0.19}$	$2.0^{+1.1}_{-1.1}$	[12]
Zw3146	0.291	$680^{+0.38}_{-0.36}$	...	1.597	$10.662^{+5.817}_{-4.577}$	[20]
				2.303	$12.592^{+5.958}_{-5.958}$	[7]
RXJ0437	0.29	...	...	2.303	$5.268^{+3.732}_{-3.732}$	[7]
RXJ0439	0.24	...	...	2.346	$14.08^{+7.15}_{-7.15}$	[7]
RXJ0451	0.430	$10.6^{+1.6}_{-1.3}$	...	0.49	$17.2^{+2.7}_{-2.1}$	[4]

Table 3 – Continued.

Cluster	$z_{\rm cluster}$	T (keV)	σ	r(Mpc)	$m(10^{14}M_{\odot})$	References
RXJ1347	0.451	$12.2^{+0.6}_{-0.6}$	1400^{+130}_{-130}	0.704	7.042	[23]
				1.408	23.94	[23]
				1.0	$14.0^{+5.0}_{-4.0}$	[17]
				$3.5^{+0.8}_{-0.2}$	$27.0^{+26.0}_{-14.0}$	[17]
				0.71	$10.0^{+0.36}_{-0.29}$	[17]
RXJ1532.9	0.345	$4.91^{+0.29}_{-0.30}$	...	1.565	$19.521^{+8.35}_{-7.94}$	[17]
RXJ1716.4+6708	0.809	$5.7^{+1.4}_{-0.6}$	...	0.35	$3.8^{+1.3}_{-0.07}$	[4]
RXJ1720.1	0.164	$5.60^{+0.50}_{-0.50}$	...	2.410	$6.56^{+4.75}_{-4.75}$	[7]
RXJ2129.6	0.235	$5.72^{+0.38}_{-0.38}$	...	2.350	$8.408^{+5.761}_{-5.761}$	[7]
Zw2089	0.24	...	...	2.346	$5.127^{+4.282}_{-4.282}$	[7]
Zw5247	0.23	...	...	2.354	$3.563^{+2.944}_{-2.944}$	[7]
Zw5768	0.27	...	...	2.32	$8.507^{+6.549}_{-6.549}$	[7]
Zw7251	0.29	...	...	2.303	$11.80^{+6.58}_{-6.58}$	[7]
1ES0657	0.296	...	1400^{+100}_{-100}	0.25	$2.8^{+0.2}_{-0.2}$	[1]

References: [1] Bradac et al. (2006); [2] Bardeau et al. (2007); [3] Cassano et al. (2007); [4] Clowe et al. (2003); [5] Cypriano et al. (2003); [6] Dahle et al. (2003); [7] Dahle (2006); [8] Diaferio et al. (2005); [9] Estrada et al. (2007); [10] Girardi et al. (2006); [11] Hoekstra et al. (1998); [12] Hoekstra et al. (2002); [13] Hoekstra (2007); [14] Horesh et al. (2005); [15] Irgens et al. (2002); [16] Johnson et al. (2006); [17] Kling et al. (2005); [18] Marshall et al. (2002); [19] Oguri et al. (2005); [20] Pedersen et al. (2007); [21] Squires et al. (1996); [22] Wu et al. (1998); [23] Zhang et al. (2005).

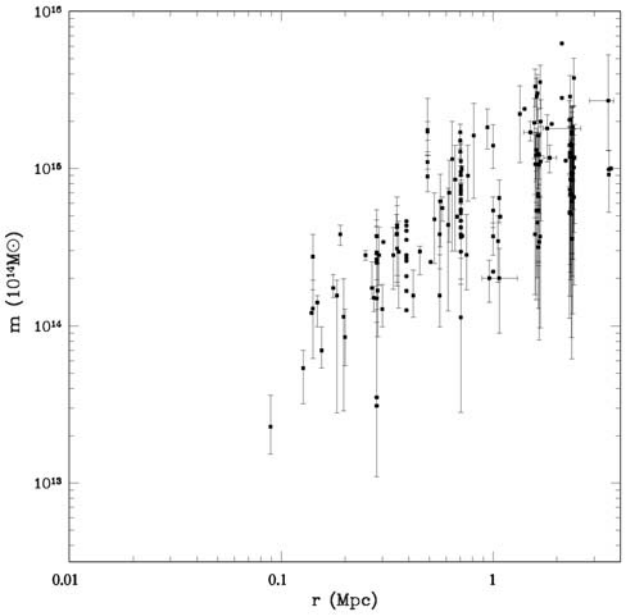

Fig. 3 Projected cluster masses given by weak lensing measurements (75 clusters).

consistent mass estimates between the modeling of giant arcs and weak lensing technique, that is indicative of a non-negligible role of complex matter structures in the interpretation of strong lensing observations.

Finally, we should point out that, when a proper normalization is taken, the overall mass profiles of all the lensing clusters agree nicely with the NFW profile revealed by numerical simulation (Navarro et al. 1995). Figure 5 shows a combination of strong lensing (modeling) and weak lensing data of all clusters, normalized by their virial radii and a certain mass fraction around $0.14r_{\rm vir}$. Superposed is the projected NFW mass profile of $r_{\rm s} = 0.19$ and $\delta_{\rm c} = 8.9 \times 10^4$ at $z = 0.3$. The significance of this agreement is that

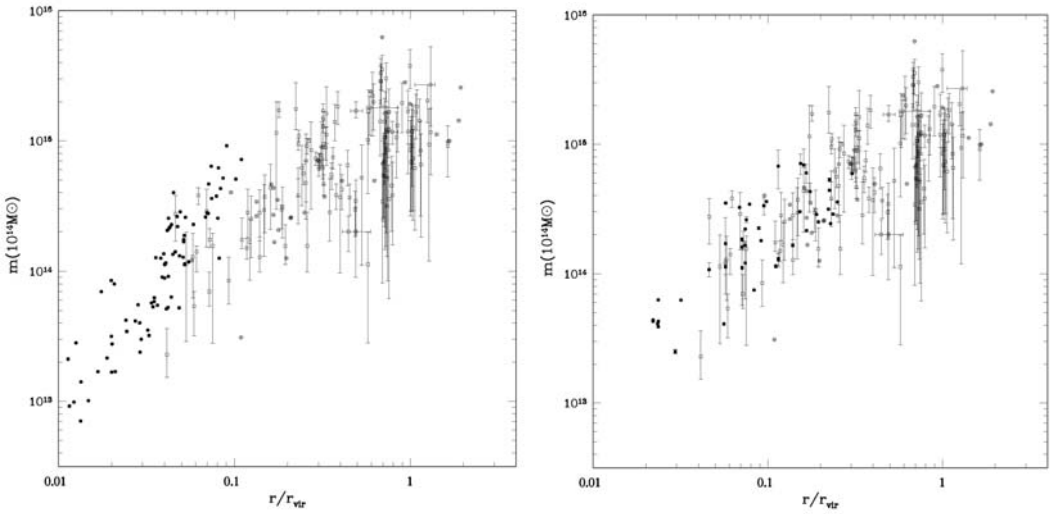

Fig. 4 Comparison of the cluster mass estimates between the fiducial model (a), modeling of arcs (b) and the weak lensing technique.

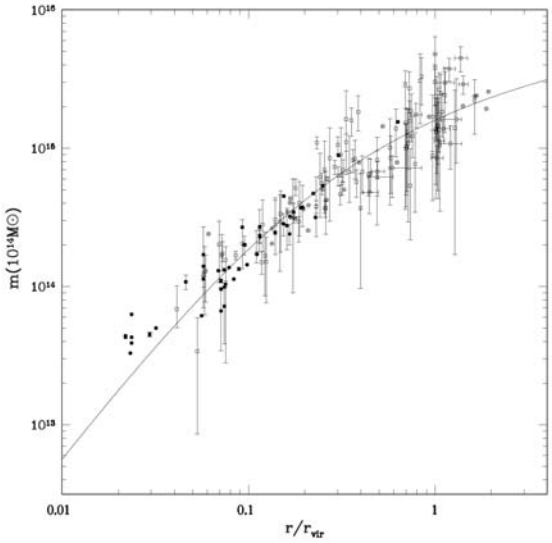

Fig. 5 Normalized cluster mass distribution given by both weak (open squares) and strong lensing (filled circles). Overlapped solid line is the projected NFW profile with $r_{\rm s} = 0.19$ and $\delta_{\rm c} = 8.9 \times 10^4$ for a choice of $\langle z \rangle = 0.3$.

the cluster data given by lensing are independent of the underlying matter content and its equation of state, and thereby provide the most reliable test for the CDM theory of structure formation.

5 CONCLUSIONS

We have performed an extensive, statistical comparison of cluster masses determined by the strong and weak gravitational lensing techniques, for a large sample of lensing clusters drawn from the literature. A systematic deviation of cluster mass estimates given by both the strong lensing and weak lensing has been

detected, and attributed to the oversimplification in the conventional strong lensing model which assumes a smooth, spherical matter distribution and that the arc traces the Einstein radius. The discrepancy will be successfully resolved if a sophisticated modeling of arc systems is employed that incorporates matter inhomogeneities, substructures and asymmetrical mass distribution along the line of sight.

It has been also noted for many years that the gravitating masses of clusters revealed by strong gravitational lensing are systematically greater than the dynamical masses estimated by X-ray gas under the assumption of hydrostatic equilibrium. However, it seems that the weak lensing and X-ray methods give a compatible cluster mass estimate at large radii, indicating that the problem may only be present in the central regions of clusters. Our ultimate aim is to solve the disagreement in the central mass, and to derive a consistent cluster mass from all cluster mass estimators, both gravitational and dynamical, fit for cosmological applications.

References

Abdelsalam H. M., Saha P., Williams L. L. R., 1998, AJ, 116, 1541
Allam S. S., Tucker D. L., Lin H. et al., 2007, ApJ, 662, L51
Allen S. W., 1998, MNRAS, 296, 392
Auger M. W., Fassnacht C. D., Abrahamse A. L. et al., 2007, AJ, 134, 668
Bardeau S., Soucail G., Kneib J.-P. et al., 2007, A&A, 470, 449
Bartelmann M., Steinmetz M., 1996, MNRAS, 283, 431
Bezecourt J., Hoekstra H., Gray M. E. et al., 2000, A&A accepted (astro-ph/0001513)
Bezecourt J., Kneib J.-P., Soucail G. et al., 1999, A&A, 347, 21
Bradac M., Clowe D., Gonzalez A. H. et al., 2006, ApJ, 652, 937
Bradac M., Schneider P., Lombardi M. et al., 2004, A&A, 423, 797
Broadhurst T., Huang X., Frye B. et al., 2000, ApJ, 534, L15
Cassano R., Brunetti G., Setti G. et al., 2007, MNRAS, 378, 1565
Campusano L. E., Pello R., Kneib J. -P. et al., 2001, A&A, 378, 394
Cavaliere A., Fusco-Femiano R., 1976, A&A, 49, 137
Coia D., McBreen B., Metcalfe L. et al., 2005, A&A, 431, 433
Clowe D., Schneider P., 2001, A&A, 379, 384
Clowe D., Luppino G.A., Kaiser N., 2003, A&A, 409, 851
Comerford J. M., Meneghetti M., Bartelmann M. et al., 2006, ApJ, 642, 39
Cypriano E. S., Lima Neto G.B., Sodre L. Jr. et al., 2005, ApJ, 630, 38
Dahle H., 2006, ApJ, 653, 954
Dahle H., Pedersen K., Lilje P. B. et al., 2003, ApJ, 591, 662
Diaferio A., Geller M. J., Rines K. J., 2005, ApJ, 628, L97
Diego J. M., Sandvik H. B., Protopapas P. et al., 2005, MNRAS, 362, 1247
Dye S., Taylor A. N., Thommas E. M. et al., 2001, MNRAS, 321, 685
Ebbels T., Ellis R., Kneib J.-P. et al., 1998, MNRAS, 295, 75
Ellis R., Allingto-Smith J., Smail I., 1991, MNRAS, 249, 184
Estrada J., Annis J., Diehl H. T., 2007, ApJaccepted (astro-ph/0701383)
Franx M., Illingworth G. D., Kelson D. D. et al., 1997, ApJ, 486, L75
Fahlman G., Kaiser N., Squires G. et al., 1994, ApJ, 437, 56
Frye B., Broadhurst T., 1998, ApJ, 499, L115
Girardi M., Boschin W., Barrena R., 2006, A&A accepted (astro-ph/0604599)
Gladders M. D., Yee H. K. C., Ellingson E., 2002, AJ, 123, 1
Gravazzi R., Fort B., Mellier Y. et al., 2003, A&A, 403, 11
Hoekstra H., 2007, MNRAS, 379, 317
Hoekstra H., Franx M., Kuijken K. et al., 1998, ApJ, 504, 636
Hoekstra H., Franx M., Kuijken K. et al., 2002, MNRAS, 333, 911
Horesh A., Ofek E. O., Maoz D. et al., 2005, ApJ, 633, 768
Irgens R. J., Lilje P. B., Dahle H. et al., 2002, ApJ, 579, 227
Johnson O., Best P., Zarisky D. et al., 2006, MNRAS, 371, 1777
Kling T. P., Dell'Antonio I., Wittman A. D. et al., 2005, astro-ph/0502281
Kneib J. P., Mellier Y., Pello R. et al., 1995, A&A, 303, 27

Lemoine-Busserolle M., Contini T., Pello R. et al., 2003, A&A, 397, 839
Limousin M., Richard J., Jullo E. et al., 2007, ApJ, 668, 643
Loeb A., Mao S., 1994, ApJ, 435, L109
Lombardi M., Rosati P., Nonino M. et al., 2000, A&A, 363,401
Marshall P. J., Hobson M. P., Gull S. F. et al., 2002, MNRAS, 335, 1037
Mellier Y., Fort B., Soucail G. et al., 1991, ApJ, 380, 334
Miralda-Escude J., Babul A., 1995, ApJ, 449, 18
Natarajan P., Kneib J. -P., Smail I. et al., 1998, ApJ, 499, 600
Navarro J. F., Frenk C. S., White S. D. M., 1995, MNRAS, 275, 720
Oguri M., Takada M., Umetsu K. et al., 2005, ApJ, 632, 841
Pedersen K., Dahle H., 2007, ApJ, 667, 26
Pello R., Le Borgne J. F., Sanahuja B. et al., 1992, A&A, 266, 6
Pierre M., Le Borgne J. F., Soucail G. et al., 1996, A&A, 311, 413
Richard J., Kneib J.-P., Jullo E. et al., 2007, ApJ, 662, 781
Rzepecki J., Lombardi M., Rosati P. et al., 2007, A&A, 741, 743
Sand D. J., Treu T., Ellis R. S., 2002, ApJ, 574, L129
Sand D. J., Treu T., Ellis R. S. et al., 2005, ApJ, 627, 32
Sand D. J., Treu T., Smith G. P. et al., 2004, ApJ, 604, 88
Saunders R., Kneissl R., Grainge K. et al., 2003, MNRAS, 341, 937
Smail I., Dickinson M., 1995, ApJ, 455, L99
Smail I., Ellis R. S., Dressler A. et al., 1997, ApJ, 479, 70
Smith G. P., Kneib J. -P., Ebeling H. et al., 2001, ApJ, 552, 493
Smith G. P., Smail I., Kneib J. -P. et al., 2002, MNRAS, 330, 1
Smith G. P., Kneib J. -P., Smail I. et al., 2005, MNRAS, 359, 417
Soucail G., Mellier Y., Fort B. et al., 1988, A&A, 191, 19
Squires G., Kaiser N., Babul A. et al., 1996, ApJ, 479, 70
Squires G., Kaiser N., Fahlman G. et al., 1996, ApJ, 469, 73
Squires G., Neumann D. M., Kaiser N. et al., 1997, ApJ, 482, 648
Taylor A. N., Dye S., Broadhurst T. J. et al., 1998, ApJ, 501, 539
Tran K. H., van Dokkum P., Illingworth G. D. et al., 2005, ApJ, 619, 134
Tyson J. A., Kochanski G. P., dell'Antonio I. P., 1998, ApJ, 498, L107
Wu X. -P., 1994, ApJ, 436, L115
Wu X. -P., Chiueh T., Fang L. -Z. et al., 1998, MNRAS, 301, 861
Wu X. -P., Fang L. -Z., 1997, ApJ, 483, 62
Wu X. -P., Hammer F., 1993, MNRAS, 262, 187
Zekser K. C., White R. L., Broadhurst T. J. et al., 2006, ApJ, 640, 639
Zhang Y. -Y., Bobringer H., Mellier Y. et al., 2005, A&A, 429, 85